Volume 10
Number 4
April 1971

Inorganic Chemistry

CONTRIBUTION FROM THE DOW CHEMICAL COMPANY,
CHEMICAL PHYSICS RESEARCH LABORATORY, MIDLAND, MICHIGAN 48640

Single-Crystal X-Ray and Raman Studies of Bis(nitrotriamminepalladium(II)) Tetraamminepalladium(II) Tetranitrate

BY F. P. BOER,* V. B. CARTER, AND J. W. TURLEY

Received August 31, 1970

The novel palladium(II)–ammine complex $[Pd(NO_2)(NH_3)_3]_2[Pd(NH_3)_4](NO_3)_4$ crystallizes in space group $I\bar{4}2m$ with unit cell dimensions of $a = 7.637$ (2) and $c = 21.610$ (5) Å and $Z = 2$. The calculated density of 2.18 g cm^{-3} is in good agreement with the observed value of 2.17 (2) g cm^{-3}. X-Ray diffraction intensity data collected on an automatic diffractometer gave a data set of 768 unique reflections which refined by least squares to a conventional R factor of 0.037. Atoms are located on sites of point symmetry $\bar{4}2m$, mm, 2, m, and 1. Analysis of the polarized Raman spectrum of oriented single crystals supports the X-ray structure, and a vibrational assignment for the crystal is proposed. The three unique Pd–NH_3 distances are 2.044 (3), 2.034 (4), and 2.053 (8) Å; the Pd–NO_2 distance is 1.984 (8) Å. N–O distances are 1.230 (6) and 1.238 (6) Å in NO_3^- and 1.104 (7) Å in the NO_2 group (1.305 Å if corrected for thermal motion). Pd shows square-planar coordination in both ions, and the packing of the nitrotriamminepalladium, tetraamminepalladium, and nitrate ions precludes any metal–metal interactions.

Introduction

In principle, the interaction of metallic palladium with nitric acid should give palladium nitrate[1] which should then react with ammonia to yield $Pd(NH_3)_4(NO_3)_2$. Instead, the investigation of this chemistry led to an almost quantitative yield of a novel complex containing the NO_2^- group,[2] for which chemical analysis gave 38.2% Pd, 26.2% N, 3.5% H, 31.7% O, 20.0% NH_3, 8.5% NO_2, and 35.0% NO_3. A preliminary crystallographic study showed that the complex crystallizes in the tetragonal system, and considerations of site multiplicities led to the formulation of the structure as the double-salt type of complex

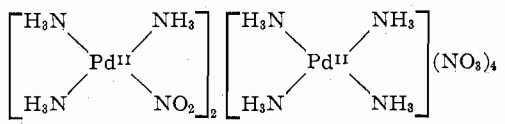

$Pd_3(NH_3)_{10}(NO_2)_2(NO_3)_4$. A single-crystal X-ray diffraction study was undertaken to verify the structure and to investigate what packing forces might be contributing to the formation of the complex. When it was realized that the solution of this highly symmetric structure must be based on the availability and interaction of symmetry sites in the lattice, the complementary study of the polarized Raman spectrum of the crystal in known orientations was initiated. A polarized Raman spectrum results from vibrations of specific symmetry species of the crystal. By correlating the symmetry of the molecular or ionic vibrations with those of the crystal, the site symmetry and orientation of the group often can be deduced. Conversely, if the crystal structure is known, the symmetry of each vibration of the molecule or ion often can be determined.

We report here the single-crystal X-ray diffraction, infrared, and Raman studies of the complex.

(1) C. C. Addison and N. Logan, *Advan. Inorg. Chem. Radiochem.*, **6**, 71 (1964).
(2) J. H. Tsai, private communication.

Experimental Section

X-Ray Data.—A sample of $[Pd(NO_2)(NH_3)_3^+]_2[Pd(NH_3)_4^{2+}][NO_3^-]_4$, mol wt 829.20, was obtained from J. H. Tsai. The crystals are bright yellow and of tabular {001} habit. A preliminary examination of the reciprocal lattice on a Weissenberg camera showed diffraction symmetry D_{4h} and the systematic absence of all reflections for which $h + k + l = 2n + 1$. Since no other systematic absences were observed, the possible space groups become $I422$ (D_4^9), $I4mm$ (C_{4v}^9), $I\bar{4}m2$ (D_{2d}^9), $I\bar{4}2m$ (D_{2d}^{11}), and $I4/mmm$ (D_{4h}^{17}). The lattice constants $a = b = 7.637 \pm 0.002$ Å and $c = 21.610 \pm 0.005$ Å were obtained by least-squares refinement of the setting angles of ten reflections on a Picker four-circle goniostat (Mo Kα radiation). The calculated density, $\rho_c = 2.184$ g cm^{-3} for $Z = 2$, agrees well with an experimental measurement of 2.17 ± 0.02 g cm^{-3}.

Intensity data were collected on a crystal of dimensions $0.979 \times 0.302 \times 0.140$ mm (parallel to a, b, and c, respectively) and aligned so that a was collinear with the ϕ axis of the diffractometer. The data were gathered using the θ–2θ scan mode of the diffractometer with Mo Kα radiation selected *via* the (0,0,2) reflection of a highly oriented graphite crystal monochromator. The takeoff angle of the X-ray tube was 4°, and an aperture 6.0 mm square was placed in front of the scintillation counter at a distance of 30 cm from the crystal. Attenuators were used to prevent the counting rate from exceeding 12,000/sec; for the

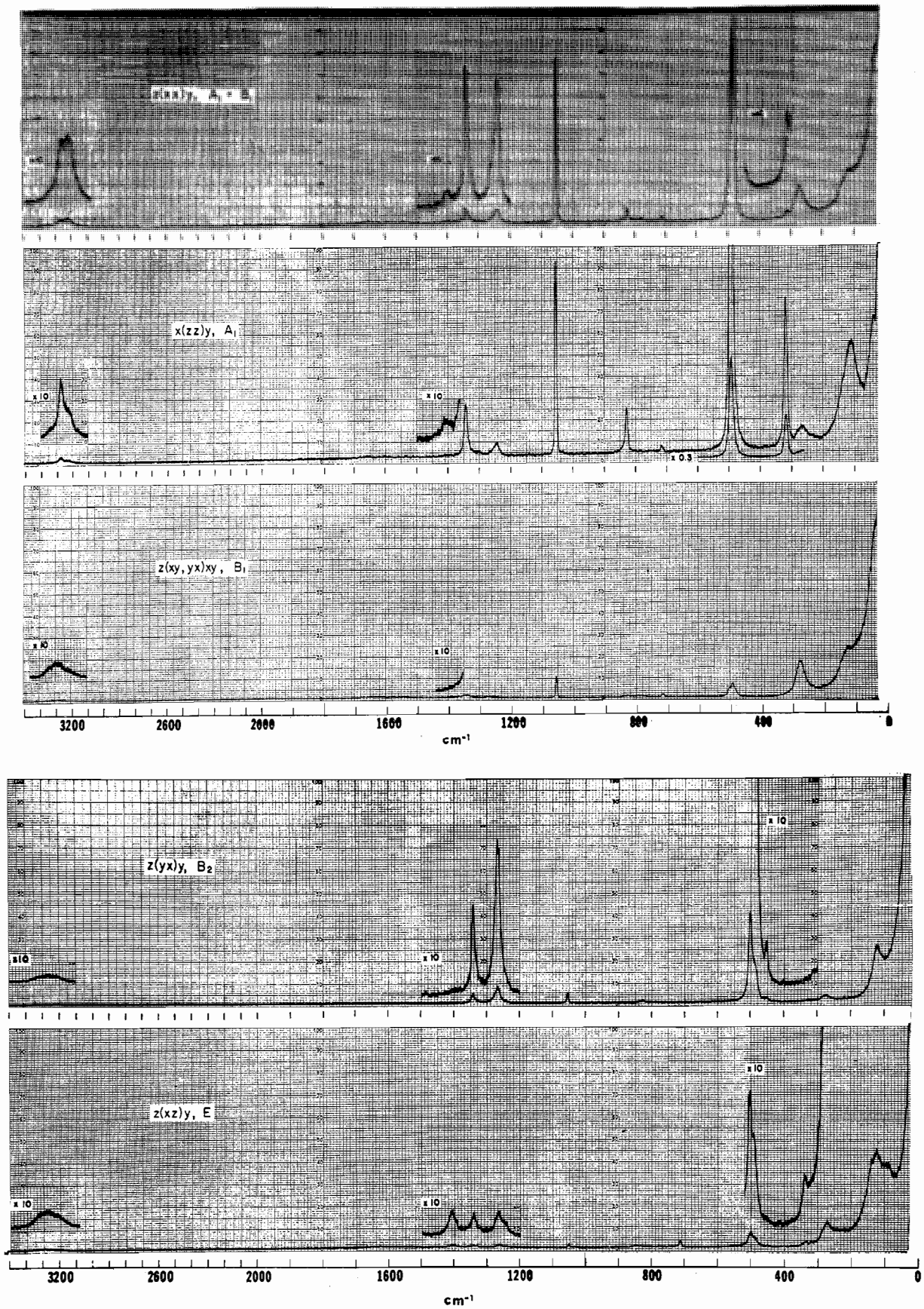

Figure 1.—Polarized Raman spectra of $[Pd(NO_2)(NH_3)_3]_2[Pd(NH_3)_4](NO_3)_4$. $z(xx)y$ denotes the direction and polarization of the light: light is incident along z polarized x (first x inside parentheses) and the scattered light is collected along y with the polarization analyzer along x (second x). For $z(xy, yx)xy$, xy and yx refer to the diagonals [110] and [1$\bar{1}$0], respectively.

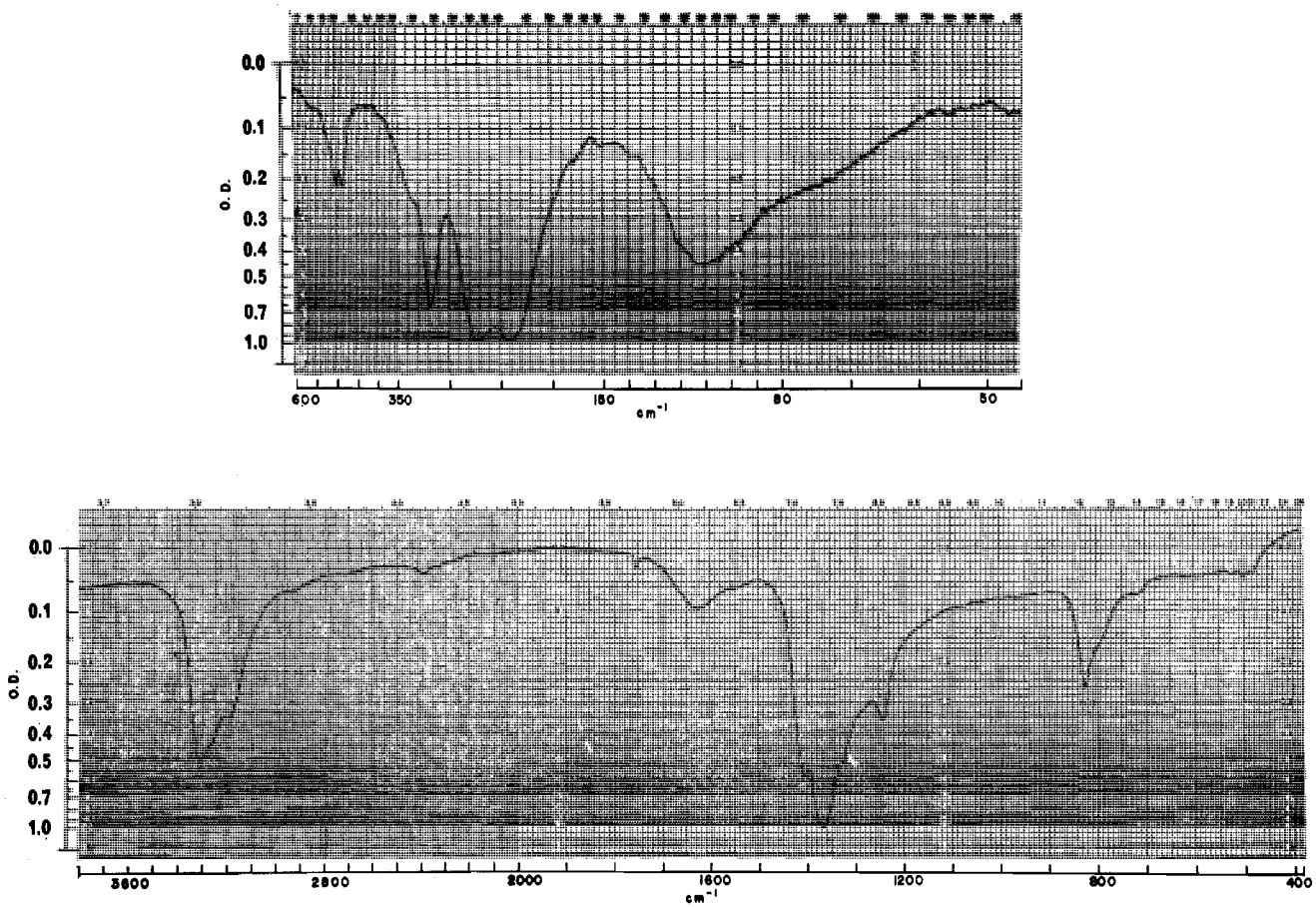

Figure 2.—Infrared spectrum of $[Pd(NO_2)(NH_3)_3]_2[Pd(NH_3)_4](NO_3)_4$ using Nujol (45–1250 cm^{-1}) and Fluorolube (1250–3800 cm^{-1}) mulls.

trongest reflections, absorbers with a total attenuation factor of 35.9 were required. Scan angles of 2.0–2.5° were used over the range (0–0.55) of sin θ examined. The scan speed was 2°/min. Stationary-crystal, stationary-counter background measurements of 10 sec were taken at each end of the scan. The (0,4,12) reflection was monitored after every 50 measurements and showed no variations in intensity greater than 1.5%.

A total of 1536 reflections were measured such that each unique reflection within the 0.55 sin θ sphere was observed at two separate symmetry-equivalent lattice points. An error $\sigma(I) = [(0.02I)^2 + N_0 + k^2N_b]^{1/2}$ was assigned to the net intensity $I = N_0 - kN_b$ in order to establish the weights $w = 4F^2/\sigma^2(F^2)$ for subsequent least-squares refinement minimizing $\Sigma w(|F_o| - |F_c|)^2$. Here N_0 is the gross count, N_b is the background count, k is the ratio of scan time to background time, and the F^2 values are the intensities corrected for Lorentz and polarization effects by the expression $Lp^{-1} = (2 \sin 2\theta)(1 + \cos^2 2\theta_m)/(1 + \cos^2 2\theta_m \cos^2 2\theta)$, where $2\theta_m$ is the monochromator setting angle. The intensity of the scattering can be judged from the fact that, of the 1536 measurements in a sphere extending to $2\theta = 67°$, there were only 47 reflections for which $I/\sigma(I)$ did not exceed 2. All reflections were included in the least-squares refinement.

An absorption correction was made using analytic formulas developed for polyhedral crystals[3] and a linear absorption coefficient $\mu = 21.6$ cm^{-1}. Transmission factors ranged from 0.50 to 0.74. The data were then merged into a single set of 738 unique reflections according to the relations $\bar{F} = (F_1F_2)^{1/2}$ and $\bar{\sigma} = (\sigma_1\sigma_2)^{1/2}$. The overall agreement was very good: an "R factor" defined as $(\Sigma|F_1 - F_2|)/(\Sigma\bar{F})$ was 0.0284. [The R factors used in least-squares refinement are given by $R_1 = \Sigma||F_o| - |F_c||/\Sigma|F_o|$ and $R_2 = \{\Sigma w(|F_o| - |F_c|)^2/(wF_o^2)\}^{1/2}$.]

(3) J. De Meulenaer and H. Tompa, *Acta Crystallogr.*, **19**, 1014 (1965). The FORTRAN program ABSCORR was written by B. Lee and V. Day and modified by K. Knox and A. D'Addario and the present authors.

Raman and Infrared Data.—The Raman spectra were measured with a Spex Ramalog using as a source of excitation a Spectra-Physics Model 125 He–Ne laser (output 55 mW at 6328 Å). The wavelength was calibrated by measuring the Ne and He emission lines prior to recording the spectra. Frequencies are accurate to approximately ±2 cm^{-1} for the sharper bands. Spectra in Figure 1 were recorded with slit widths of 375 μ (~5-cm^{-1} resolution) and scan speeds of 250 and 50 cm^{-1}/min. Crystals of approximate dimensions 2 × 4 × 0.5 mm, with faces perpendicular to the desired crystal axes, were used in these measurements. For each crystal orientation used, the instrument sensitivity was adjusted so that band intensities resulting from off-diagonal terms of the polarizability derivative tensor remained approximately the same. Relatively weak or overlapping bands in these spectra result in intensities which are only roughly comparable. Each spectrum contains bands belonging to species other than the one measured, due possibly to depolarization of the light resulting from slight crystal misalignment or imperfect crystal faces.

Infrared spectra of the polycrystalline solid (Nujol and Fluorolube mulls) were recorded using a Herscher-Dow KBr foreprism-grating spectrometer[4] (3800–400 cm^{-1}) and a Beckman IR-11 spectrometer (600–45 cm^{-1}). The spectra are shown in Figure 2.

Solution and Description of the Structure

Certain problems originating in the high symmetry of the crystal made the determination of this structure an interesting exercise. Because the details are essential to an understanding of the final model, we will review the solution and refinement of this structure somewhat more fully than usual.

(4) L. W. Herscher, *Spectrochim. Acta*, **15**, 901 (1959).

The space group could be deduced only after analysis of the Patterson function,[5] although the choice was narrowed by symmetry considerations. If the hydrogen atoms are ignored, the $Pd(NO_2)(NH_3)_3^+$ ion can occupy sites of point symmetry 1, 2, *m*, or *mm*, but none higher. Because space groups $I422$ or $I4/mmm$ have[6] neither a fourfold special position nor any combination of twofold positions that satisfy this requirement, these groups can be eliminated for ordered structures. A symmetry-allowed solution exists for $I4mm$: $Pd(NH_3)_4^{2+}$ on 2a sites, $Pd(NO_2)(NH_3)_3^+$ on 4b, and NO_3^- at either 8c or 8d positions.[6] However, this solution demands a large Pd–Pd interaction at $(1/2, 1/2, 0)$ in the Patterson map. $I4mm$ was ruled out because this vector did not appear, and because this solution failed to account for the largest nonorigin peak in the Patterson, that at (0, 0, 0.259).

The choice is then between $I\bar{4}m2$ and $I\bar{4}2m$, both of which can accommodate the $Pd(NH_3)_4^{2+}$ ion in twofold positions of point symmetry $\bar{4}2m$ and the $Pd(NO_2)(NH_3)_3^+$ ions in fourfold positions of *mm* symmetry in a manner that accounts for the Pd–Pd interactions in the Patterson map. The two possibilities can be easily distinguished by noting that the NH_3 groups of the $Pd(NH_3)_4^{2+}$ ion must lie on mirror planes, if this ion is to occupy a $\bar{4}2m$ site. In space group $I\bar{4}m2$, the mirrors parallel the cell edges, and in $I\bar{4}2m$ they are diagonal. The Patterson function clearly showed the Pd–NH_3 vectors on the diagonals, thus establishing $I\bar{4}2m$ (D_{2d}^{11}). These positions were confirmed in subsequent Fourier maps.

A structure factor calculation[7] was performed assuming two Pd atoms at the 2a ($\bar{4}2m$) positions and four Pd atoms at the 4e (*mm*) sites, with coordinates (0, 0, 0.259). The R values for the heavy atoms alone were $R_1 = 0.192$ and $R_2 = 0.357$. An electron density map[5] based on the Pd phases showed the essential features of the structure with the addition of a false center of symmetry at $(1/4, 1/4, 1/4)$ that left the effective space group as $I4/mmm$. Several of the light atoms appeared in the Fourier map at special positions that were unaffected by this ambiguity. In this category were N(3) and N(4) in 4e positions and O(2) and N(5) at 8h positions. Of course these atoms could be of no help in breaking the false center. The nitrogen atoms N(1) of the $Pd(NH_3)_4^{2+}$ ions lie in 8i positions (x, x, z) of $I\bar{4}2m$, which in general are not related by the false center. However, because this ion is planar, the *z* coordinate of N(1) is required to be very close to zero, where it falls on the 8h positions of $I4/mmm$. Thus, N(1) also fails to aid in resolving the false center. A similar situation occurs for O(3). This atom lies in a general (16j) position of $I\bar{4}2m$, but its coordinates place it nearly at $(1/2, y, z)$, a 16n (symmetry *m*) position of $I4/mmm$. In fact, its Fourier peak falls on the false mirror plane in the map at $x = 1/2$, and its x coordinate only moves off this plane on refinement. This atom is also of little use in breaking the false symmetry.

The remaining atoms are N(2) and O(1), on the (x, x, z) mirrors (8i positions). The false center was broken by arbitrarily assigning one of these atoms, N(2), to the positive quadrant. The ambiguity was then reduced to the choice of quadrant for the oxygen atom O(1) of the NO_2 group: the plane of this group could be aligned either parallel to the {Pd(2), N(2), N(2)′, N(3)} plane, on the (x, x, z) mirror, or perpendicular to it, on the $(x, \bar{x}, z)$ mirror. These two sites are equivalent in space group $I4/mmm$. Not surprisingly, then, an electron density map based on all of the other atoms gave peaks at both sites. However, when O(1) was placed at either of the two possible locations, a peak always appeared at the other site in the electron density difference maps. A similar residual at the unoccupied site was *not* shown by N(2). A preference for the parallel site appeared upon refinement: three-cycles of least-squares assuming isotropic thermal parameters for all atoms gave $R_1 = 0.0818$ and $R_2 = 0.1115$ for O(1) at (x, x, z) and $R_1 = 0.0838$ and $R_2 = 0.1180$ for O(1) at $(x, \bar{x}, z)$. The ratio of the R_2 factors $\mathcal{R} = 1.058$ exceeds $\mathcal{R}_{3,743,0.005} = 1.0089$, and the parallel sites appear to be preferred at the 0.005 significance level.[8] However, this analysis does not take into account the possibility of disorder between the two positions of O(1), a situation that appears plausible in view of the high temperature factor exhibited by this atom. Although a reliable refinement of relative occupancy factors of the two sites cannot be made in view of the fact that the two positions are coupled through the false center of symmetry, a structure factor calculation assigning 50% occupancy factors for each site gave a ratio R_2(disordered)/R_2(ordered, parallel) of 1.056, again favoring the parallel model. Thus, we decided to continue refinement assuming O(1) to be localized at the parallel sites.

At this point, three strong reflections[9] that seemed to be affected by secondary extinction were removed from the data set. Also, a correction[10] was introduced for the real and imaginary components of anomalous scattering by Pd. Because the structure was very close to a centrosymmetric one, no attempt was made to distinguish between $F(hkl)$ and $F(\bar{h}\bar{k}\bar{l})$ at this time. After two more cycles of isotropic least squares (25 variables, 765 observations) R_1 was reduced to 0.080 and R_2 to 0.111. Final values for the isotropic temperature factors (Å^2) were as follows: Pd(1), 2.43 ± 0.03; Pd(2), 2.18 ± 0.03; N(1), 3.36 ± 0.18; N(2), 3.63 ± 0.27; N(3), 4.18 ± 0.35; N(4), 4.91 ± 0.44; O(1), 10.33 ± 0.70; O(2), 5.85 ± 0.31; O(3), 6.23 ± 0.25.

In our first effort to vary anisotropic thermal parameters, using the set of symmetry constraints on the x,

(5) J. Gvildys, "Two- and Three-Dimensional Crystallographic Fourier Summation Program," based on MIFRI, Program Library B-149, Argonne National Laboratory, Applied Mathematics Division, April 13, 1965 (CDC-3800).

(6) See the "International Tables for X-Ray Crystallography," Vol. I, Kynoch Press, Birmingham, England, 1962.

(7) J. Gvildys, "A Fortran Crystallographic Least-Squares Refinement Program," based on ORFLS, Program Library 14E7043, Argonne National Laboratory, Applied Mathematics Division, March 31, 1967 (CDC3800).

(8) W. C. Hamilton, *Acta Crystallogr.*, **18**, 502 (1965).

(9) These were 020 (F_o = 891, F_c = 1115), 220 (F_o = 942, F_c = 1040), 040 (F_o = 616, F_c = 697).

(10) Scattering factors used were: (a) $f_o(Pd^{2+})$: D. T. Cromer and J. T. Waber, *Acta Crystallogr.*, **18**, 104 (1965); (b) $\Delta f'$(Pd), $\Delta f''$(Pd): "International Tables for X-Ray Crystallography," Vol. III, Kynoch Press, Birmingham, England, 1962, p 216; (c) f_o(N), f_o(O): *ibid.*, pp 201–203.

TABLE I

OBSERVED AND CALCULATED STRUCTURE FACTORS FOR BIS(NITROTRIAMMINEPALLADIUM(II)) TETRAAMMINEPALLADIUM(II) NITRATE

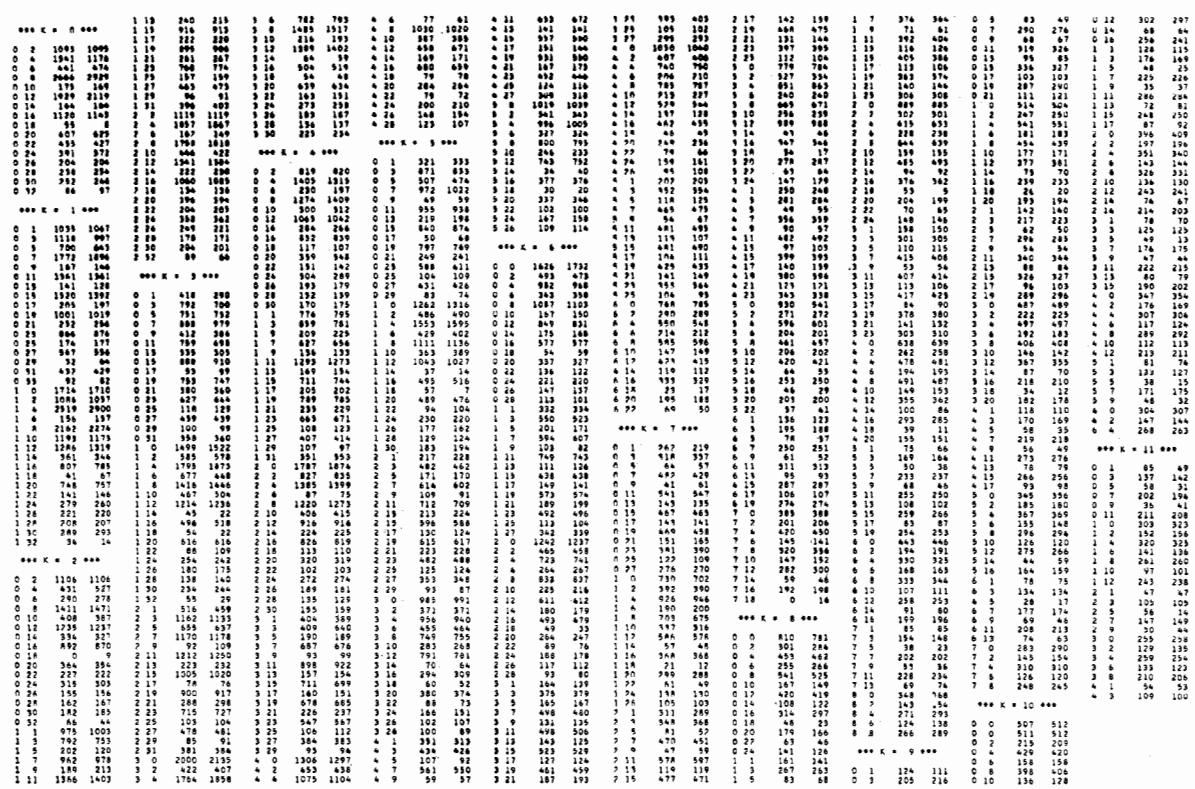

y, z's and β_{ij}'s appropriate[11] to space group $I\bar{4}2m$, the program terminated refinement after one cycle when the requirement $\beta_{12}^2 \geq \beta_{11}\beta_{22}$ was violated for atom N(3). In fact, several other β_{12} values appeared to be unusually high, and an examination of the correlation matrix also showed large coefficients (from -0.52 to 0.39) among the β_{12} terms. We noted, however, that in the centrosymmetric space group $I4/mmm$, atoms in the special 4e and 8g positions have the constraint $\beta_{12} = 0$ in addition to the normal constraints applying to 4e and 8h positions of $I\bar{4}2m$. This consideration led us to postulate that the close resemblance of the structure to $I4/mmm$ leads to an ill-conditioned matrix when the β_{12}'s of the 4e (Pd(2), N(3), N(4)) and 8h (N(5), O(2)) atoms are varied. Accordingly, we set these terms to zero, and with these additional constraints five cycles of full-matrix anisotropic refinement proceeded smoothly to final values of 0.037 for R_1 and 0.051 for R_2 (765 observations, 47 variables). Structure factors calculated from the final parameter set are compared with observed values in Table I. The R factor ratios for choice of enantiomer were calculated but were inconclusive. The most significant differences occurred for the (1,1,6) and (2,2,6) reflections $\{$(1,1,6): $F_c/F_o = 0.90$, $F_c^i/F_o = 1.19$; (2,2,6): $F_c/F_o = 0.97$, $F_c^i/F_o = 1.23\}$, both of which favor the chosen enantiomer.

We also examined the question whether the true space group was indeed $I4/mmm$. The $I4/mmm$ model requires both N(2) and O(1) to be disordered in 16m positions and places N(1) in the 8h positions at $(x, x, 0)$ and O(3) into 16n positions at $x = 1/2$. In view of the possible disorder of O(1) and the fact that only small changes in position occur for N(1) and O(3), the major difference is the assumption of disorder for N(2). Least-squares refinement in $I4/mmm$ gave $R_1 = 0.048$ and $R_2 = 0.082$ after five cycles (765 observations, 42 variables). The R_2 factor ratio $\mathcal{R} = 0.082/0.051$ is 1.61 and thus strongly favors the $I\bar{4}2m$ model. In addition, the two independent N–O distances of the nitrate ion agreed poorly in the $I4/mmm$ refinement, and a substantially wider variation in Pd–NH_3 distances occurred.

By restricting certain β_{12} terms to zero, we have imposed some constraints on the form of the thermal ellipsoids[12] of those atoms. For atoms in the 4e positions of $I\bar{4}2m$, the usual conditions are $\beta_{11} = \beta_{22}$ and $\beta_{23} = \beta_{13} = 0$, which give principal axes of length $[(\beta_{11} + \beta_{12})/2\pi^2 a^{*2}]^{1/2}$ along [110], $[(\beta_{11} - \beta_{12})/2\pi^2 a^{*2}]^{1/2}$ along $[1\bar{1}0]$, and $[\beta_{33}/2\pi^2 c^{*2}]^{1/2}$ along [001]. These solutions are, of course, compatible with the diagonal mirror planes intersecting at (0, 0, z) in $I\bar{4}2m$. Space group $I4/mmm$ imposes the constraint $\beta_{12} = 0$, resulting in degenerate solutions for the first two principal axes. Essentially, the fourfold axis reduces the original ellipsoid to a spheroid of rotation on c. The situation is somewhat different at the 8h positions, where the conditions of $I\bar{4}2m$ are those of a diad in the c direction; *i.e.*, $\beta_{13} = \beta_{23} = 0$. One axis of the thermal ellipsoid will again be

(11) W. J. A. M. Peterse and J. H. Palm, *Acta Crystallogr.*, **20**, 147 (1966).

(12) J. Waser, *ibid.*, **8**, 731 (1955).

TABLE II

FINAL ATOMIC PARAMETERS FOR $[Pd(NH_3)_3(NO_2)]_2[Pd(NH_3)_4](NO_3)_4$[a,b]

Atom	Wyckoff set	x	y	z	β_{11}	β_{22}	β_{33}	β_{12}	β_{13}	β_{23}
Pd(1)	2a	0	0	0	1282 (9)	β_{11}	87 (1)	0	0	0
Pd(2)	4e	0	0	0.25959 (2)	957 (7)	β_{11}	115 (1)	0[c]	0	0
N(1)	8i	0.1892 (6)	x	0.0007 (5)	1711 (64)	β_{11}	187 (11)	−311 (91)	−123 (63)	β_{13}
N(2)	8i	0.1883 (7)	x	0.2601 (4)	1418 (76)	β_{11}	258 (19)	−468 (104)	0 (26)	β_{13}
N(3)	4e	0	0	0.3546 (4)	2542 (136)	β_{11}	109 (12)	0[c]	0	0
N(4)	4e	0	0	0.1678 (4)	2323 (125)	β_{11}	125 (14)	0[c]	0	0
N(5)	8h	0.5	0	0.1217 (2)	1661 (112)	1585 (107)	160 (10)	0[c]	0	0
O(1)	8i	0.0863 (12)	x	0.1404 (3)	9920 (508)	β_{11}	157 (13)	−6172 (579)	182 (50)	β_{13}
O(2)	8h	0.5	0	0.1790 (3)	3299 (187)	3400 (196)	161 (9)	0[c]	0	0
O(3)	16j	0.5125 (20)	0.1379 (7)	0.0927 (2)	2615 (148)	2244 (94)	373 (13)	297 (214)	−103 (52)	345 (32)

[a] Standard errors are given in parentheses. [b] The anisotropic temperature factors, given in the form $\exp[-(\beta_{11}h^2 + \beta_{22}k^2 + \beta_{33}l^2 + 2\beta_{12}hk + 2\beta_{13}hl + 2\beta_{23}kl)]$, are multiplied by 10^5. [c] Set equal to zero. See text.

TABLE III

ROOT-MEAN-SQUARE AMPLITUDES (Å) OF VIBRATION AND DIRECTION COSINES FOR $[Pd(NO_2)(NH_3)_3]_2[Pd(NH_3)_4](NO_3)_4$

Atom	Minor axis	Intermed axis	Major axis
Pd(1)	0.144	0.195	0.195
	(0, 0, 1)	(1, 0, 0)	(0, 1, 0)
Pd(2)	0.165	0.168	0.168
	(0, 0, 1)	(1, 0, 0)	(0, 1, 0)
N(1)	0.168	0.240	0.244
	(0.524, 0.524, 0.671)	(−0.474, −0.474, 0.741)	(0.707, −0.707, 0)
N(2)	0.168	0.236	0.247
	(0.707, 0.707, 0)	(0.707, −0.707, 0)	(0, 0, 1)
N(3)	0.161	0.274	0.274
	(0, 0, 1)	(1, 0, 0)	(0, 1, 0)
N(4)	0.172	0.262	0.262
	(0, 0, 1)	(1, 0, 0)	(0, 1, 0)
N(5)	0.195	0.216	0.222
	(0, 0, 1)	(0, 1, 0)	(1, 0, 0)
O(1)	0.176	0.341	0.690
	(−0.184, −0.184, 0.965)	(0.683, 0.683, 0.261)	(0.707, −0.707, 0)
O(2)	0.195	0.312	0.317
	(0, 0, 1)	(1, 0, 0)	(0, 1, 0)
O(3)	0.205	0.285	0.329
	(0.328, −0.772, 0.544)	(0.942, 0.313, −0.123)	(−0.075, 0.553, 0.830)

directed along [001] with rms amplitude $[\beta_{33}/2\pi^2c^{*2}]^{1/2}$. The other two axes will have amplitudes

$$\frac{\beta_{11} + \beta_{22} \pm \sqrt{(\beta_{11} - \beta_{22})^2 + 4\beta_{12}^2}}{2a^{*2}}$$

and will be oriented at respective angles to [100] of

$$\tan^{-1}\left\{\frac{\beta_{11} - \beta_{22} \mp \sqrt{(\beta_{11} - \beta_{22})^2 + 4\beta_{12}^2}}{2\beta_{12}}\right\}$$

These solutions allow principal axes of arbitrary length in any two directions orthogonal simultaneously to each other and to [001]. For $\beta_{12} = 0$, however, the equations reduce to give principal axes of length $[\beta_{11}/2\pi^2a^{*2}]^{1/2}$ along [100] and $[\beta_{22}/2\pi^2a^{*2}]^{1/2}$ along [010], which are, of course, compatible with the two mirror planes that intersect at these sites in $I4/mmm$. An alternative method of refining the 8e atoms might be to consider them as spheroids of revolution ($\beta_{11} = \beta_{22}$). Since our refinement gave $\beta_{11} \approx \beta_{22}$, there appeared to be little practical difference between the approximation used and this spheroid model.

Atomic parameters and their standard errors obtained in the final least-squares cycle are given in Table II; the corresponding root-mean-square amplitudes of vibration are in Table III. In the final cycle no parameter shifted more than 0.13σ, and the average shift was only 0.30σ. In a final difference Fourier map, the largest residuals were peaks of height 0.8 $e^-/Å^3$ at O(1) and of 1.1 $e^-/Å^3$ at the centrosymmetric image of O(1), *i.e.*, the $(x, x, \bar{z})$ position discussed above.

Discussion

The crystal contains nitrotriamminepalladium and tetraamminepalladium ions in a 2:1 ratio; both the single-crystal Raman data and the X-ray structure agree on the orientation of these ions in the unit cell. The 318-cm^{-1} Raman band is strong only in the α_{zz} polarization (A_1) and is the most intense band below 490 cm^{-1}. This band is readily identified as the Pd–NO_2 stretching mode with the bond direction along the z axis. This result is substantiated by the X-ray structure which shows the nitrotriamminepalladium ions lying in the (110) planes with the Pd–NO_2 bond directed along z. The location of the tetraamminepalladium ions in the (001) planes with the nitrogen atoms placed on the cell diagonals rather than the edges is consistent with the factor group components of the Pd–NH_3 stretching mode and the NH_3 symmetric deformation $A_1 + B_2 + E$, rather than $A_1 + B_1 + E$ (Table IV).

TABLE IV

VIBRATIONAL SPECTRA OF CRYSTALLINE $[PdNO_2(NH_3)_3]_2[Pd(NH_3)_4](NO_3)_4$

Ir	Raman						Crystal symmetry		
	α_{xx}	α_{zz}	α_{xx-yy}	α_{xy}	α_{xz}				
$B_2 + E$	$A_1 + B_1$	A_1	B_1	B_2	E	Description	$Pd(NH_3)_4^{2+}$	$Pd(NH_3)_3NO_2^+$	NO_3^-
					90 sh	Lattice modes	$3A_1 + 4A_2 + 3B_1 + 3B_2 + 13E$		
112 w		112 m				N–Pd–N out-of-plane bends	$A_1 + B_2$	2 E	
	122 w		122 w	122 w	122 m				
240 w						N–Pd–N in-plane bends	$B_1 + E$	$A_1 + B_2 + 2E$	
		268 w							
273 w					272 w	NO_2 $\rho_r(b_2)$, $\rho_t(b_1)$		E, E	
	278 w		278 w	278[a]					
318 w	318[a]	318 s				Pd–NO_2 $\nu(a_1)$		$A_1 + B_2$	
338 sh					337 vw				
				452 vw	452[a]				
483 vw									
	490 s	490 s	490[a]	490[a]	490[a]	Pd–NH_3 $\nu(a_1)$	$A_1 + B_2 + E$	$2A_1 + 2B_2 + E$	
500 vw						NO_2 $\rho_w(b_1)$		E	
				502 ms	502[a]				
524 sh									
555 sh									
712 vw	714 vw	714 vw	714 vw		714 vw	NO_3^- $\delta_d(e')$			$A_1 + A_2 + B_1 + B_2 + 2E$
790 sh						NH_3 $\delta_r(e)$	$A_1 + A_2 + B_1 + B_2 + 2E$	$A_1 + A_2 + B_1 + B_2 + 4E$	
824 m	827 w	827 m	827[a]	827 (?)		NO_2 $\delta(a_1)$		$A_1 + B_2$	
829 sh						NO_3^- $\pi(a_2'')$			2 E
	1053 s	1053 s	1053 w	1053[a]	1053[a]	NO_3^- $\nu_s(a_1')$			$A_1 + A_2 + B_1 + B_2$
1243 m	1243 w	1243 w							
				1267 w	1267[a]	NH_3 $\delta_s(a_1)$	$A_1 + B_2 + E$	$2A_1 + 2B_2 + E$	
1285 sh									
1341 sh	1341 w	1341 m	1341[a]	1341 w	1341[a]	NO_2 $\nu_s(a_1)$		$A_1 + B_2$	
1368 vs									
	1402 vw					NO_3^- $\nu_{as}(e')$			$A_1 + A_2 + B_1 + B_2 + 2E$
1408 s		1408 (?)			1408 vw	NO_2 $\nu_{as}(b_2)$		E	
1550 sh									
1628 m						NH_3 $\delta_d(e)$	$A_1 + A_2 + B_1 + B_2 + 2E$	$A_1 + A_2 + B_1 + B_2 + 4E$	
1753 w						NO_3^- $\nu_d + \delta_d(e')$			
3198 sh									
	3209 vw	3209 vw							
3260 sh						NH_3 $\nu_s(a_1)$	$A_1 + B_2 + E$	$2A_1 + 2B_2 + E$	
	3271 vw	3271 vw							
			3295 (?)			NH_3 $\nu_{as}(e)$	$A_1 + A_2 + B_1 + B_2 + 2E$	$A_1 + A_2 + B_1 + B_2 + 4E$	
3312 s									
					3326 vvw				

[a] Band believed to belong to a different symmetry class.

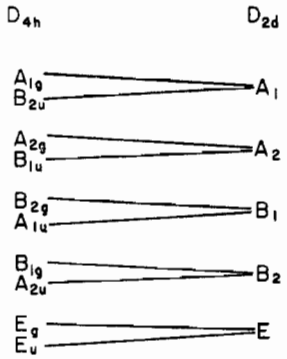

Figure 3.—Correlation diagram for $Pd(NH_3)_4^{2+}$; site and crystal symmetry are both D_{2d}.

The $Pd(NH_3)_4^{2+}$ ion is on a D_{2d} site in the crystal with one ion in the primitive cell (Figure 3). Nine skeletal modes of vibration occur: four metal–nitrogen stretching modes (a_{1g}, b_{1g}, and e_u) and five bending modes (in plane, b_{2g} and e_u; out of plane, a_{2u} and b_{2u}). The $Pd(NO_2)(NH_3)_3^+$ ion is on a C_{2v} site with two ions in the primitive cell (Figure 4). This ion also has nine skeletal

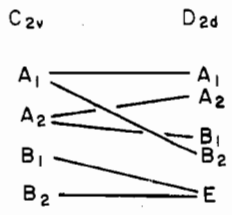

Figure 4.—Correlation diagram for $Pd(NO_2)(NH_3)_3^+$ and NO_2; point group and site symmetry are both C_{2v}.

modes: four stretching modes (3 a_1 and b_2) and five bending modes (in plane, a_1 and 2 b_2; out of plane, 2 b_1). If we assume no mixing between the skeletal modes of the complex and the internal modes of the ligand, the

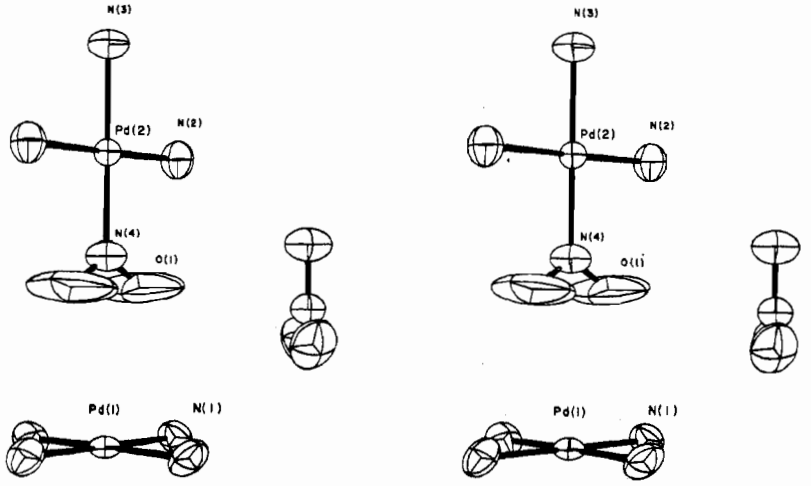

Figure 5.—A stereoview of the three ions in $[Pd(NO_2)(NH_3)_3]_2[Pd(NH_3)_4](NO_3)_4$.

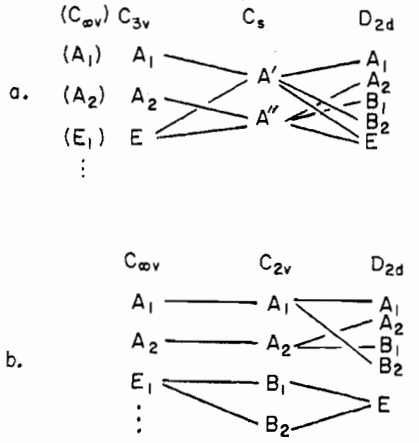

Figure 6.—Correlation diagram for NH_3: (a) groups for $Pd(NH_3)_4^{2+}$ and groups cis to NO_2 for $Pd(NO_2)(NH_3)_3^+$; (b) group trans to NO_2.

ligands can be treated separately in the analysis of the polarized Raman spectrum.

The NH_3 ligands.—There are three unique Pd–NH_3 bonds in the structure (see Figure 5), but the Pd(1)–N(1) distance of 2.044 (3) Å in the $Pd(NH_3)_4^{2+}$ ion, the Pd(2)–N(2) distance of 2.034 (4) Å in the $Pd(NH_3)_3(NO_2)^+$ ion, and the Pd(2)–N(3) distance of 2.053 (8) Å (trans to the $-NO_2$ ligand) cannot be considered to differ significantly (Table V). These values are in close

TABLE V
BOND DISTANCES AND ANGLES IN $[Pd(NH_3)_3(NO_2)]_2[Pd(NH_3)_4](NO_3)_4$[a,b]

Distances, Å			
Pd(1)–N(1)	2.044 (3)	N(4)–O(1)	1.104 (7)
Pd(2)–N(2)	2.034 (4)	N(5)–O(2)	1.238 (6)
Pd(2)–N(3)	2.053 (8)	N(5)–O(3)	1.230 (6)
Pd(2)–N(4)	1.984 (8)		
Angles, Deg			
N(1)–Pd(1)–N(1)′	179.2 (6)	Pd(2)–N(4)–O(1)	122.4 (5)
N(1)–Pd(1)–N(1)″	89.6 (3)	O(1)–N(4)–O(1)′	115.2 (9)
N(2)–Pd(2)–N(2)′	179.4 (4)	O(1)–Pd(1)–O(1)′	34.2 (2)
N(2)–Pd(2)–N(3)	89.7 (2)	O(2)–N(5)–O(3)	120.7 (3)
N(2)–Pd(2)–N(4)	90.3 (2)	O(3)–N(5)–O(3)	118.6 (6)

[a] Primed atoms are related by diads; double primed by $\bar{4}$ axes. [b] Standard errors were computed from the variance–covariance matrix obtained in the final least-squares cycle.

agreement with bond distances of 2.030 and 2.043 Å reported for bis(ethylenediamine)palladium(II) chloride[13] and are in the range of other Pd–N values in the literature[14–16] (2.00–2.09 Å).

The Pd–NH_3 stretching modes are expected to give bands in the region from about 400 to 540 cm^{-1} (Table VI).[17–22] By comparison of the spectrum with that of $[Pd(NH_3)_4]Cl_2$,[21] bands at 491 (A_1) and 452 cm^{-1} (B_2) are assigned as the a_{1g} and b_{1g} stretching modes of $Pd(NH_3)_4^{2+}$, respectively. For $Pd(NO_2)(NH_3)_3^+$ the Pd(2)–N(2) symmetric (a_{1g}) mode can then be assigned to the 491 (A_1) and 502 cm^{-1} (B_2) bands and the Pd(2)–N(3) (a_{1g}) mode to the 491 cm^{-1} (A_1) band. Since only one band was measured in the A_1 spectra (both α_{xx} and α_{zz} polarization), all three A_1 modes are assumed to have the same frequency, within the limit of our experiment. The B_2 factor group component of the Pd(2)–N(3) stretching mode is not expected to give a strong band in the Raman spectrum since the bond direction is along the z axis and, therefore, was not assigned. The only bands recorded in this region in the α_{xz} spectrum (E) are probably the A_1 and B_2 modes; the intensity of these bands varied with alignment of the sample and the condition of the crystal faces. Four bands occur in the infrared spectrum (B_2 and E) in the region 400–700 cm^{-1}: at 483, 500, 524, and 555 cm^{-1}. Those Pd–NH_3 stretching modes which can be expected to have large dipole moment changes are the e_u mode of $Pd(NH_3)_4^{2+}$, the b_2 mode of Pd(2)–N(2), and the B_2 factor group component of the a_{1g} mode of Pd(2)–N(3), mentioned above. The B_2 components measured in the Raman spectrum involve motions largely in the xy plane and would not be expected to give large dipole moment changes (B_2, T_z). Therefore, at least three of the four bands in this region of the infrared spectrum appear to result from the Pd–NH_3 stretching vibration; the fourth (555 cm^{-1}) may be either the wagging mode of the nitro group (E) (see below) or a Pd–NH_3 stretching mode.

An ammine group has nine modes of vibration, three stretching modes (a_1 and e), three deformations (a_1 and e), two rocking modes (e), and a twisting mode (Figure 6). With ten NH_3 ligands in the primitive cell, the number of discrete bands allowed for each vibrational mode is quite large. However, the number actually measured in either the Raman or the infrared spectrum is much smaller. Three infrared and four Raman bands are measured in the N–H stretching region. The asymmetric deformation is assigned to the broad infrared

(13) J. R. Wiesner and E. C. Lingafelter, *Inorg. Chem.*, **5**, 1770 (1966).
(14) V. W. Day, M. D. Glick, and J. L. Hoard, *J. Amer. Chem. Soc.*, **90**, 4803 (1968).
(15) D. J. Robinson and C. H. L. Kennard, *Chem. Commun.*, 1236 (1967).
(16) O. Hassel and B. F. Pedersen, *Proc. Chem. Soc., London*, 394 (1959).
(17) K. Nakamoto, J. Fujita, and H. Murata, *J. Amer. Chem. Soc.*, **80**, 4817 (1958).
(18) M. J. Cleare and W. P. Griffith, *J. Chem. Soc. A*, 1144 (1967).
(19) J. S. Coe, R. Hulme, and A. A. Malik, *ibid.*, 138 (1964).
(20) J. Hiraishi, J. Nakagawa, and T. Shimanouchi, *Spectrochim. Acta, Part A*, **24**, 819 (1968).
(21) P. J. Hendra, *ibid., Part A*, **23**, 1275 (1967).
(22) J. R. Durig and D. W. Wertz, *Appl. Spectrosc.*, **22**, 627 (1968).

TABLE VI

COMPARISON OF VIBRATIONAL SPECTRA OF $[Pd(NO_2)(NH_3)_3]_2[Pd(NH_3)_4](NO_3)_4$ AND SIMILAR COMPLEXES

	$Pt(NO_2)_4^{2-}$ [16]	$K_2[Pt(NO_2)Cl_3]$ [17] (ir)		$[Pd(NO_2)(NH_3)_3]Cl$ [18] (ir)[a]	M–NO_2 [21]	$[Pd(NO_2)(NH_3)_3]_2$-$[Pd(NH_3)_4](NO_3)_4$
$\nu(NO_2)$	1440 (ir), 1410 (R), 1335 (ir), 1360 (R)	1401, 1325		1450, 1390, 1350	1345–1497 (ν_a) 1300–1373 (ν_s)	1408–1341
$\delta(NO_2)$	833 (ir), 835 (R)	844		770–850	798–849	790–829
$\rho_w(NO_2)$	636, 613 (ir)	614		530 (?)	550–650	555 (?)
ν(M–N)	450 (ir), 319, 307 (R)	350		310 (?)	275–450	318
MN bend	245 (R)			270–330		
$\rho_r(NO_2)$	185 (R)	304		270–330	250–300	
Other bands		323, 316			ρ_t unobsd	
	$[Pt(NH_3)_4]Cl_2 \cdot H_2O$ [19] (ir)	$[Pd(NH_3)_4]$-$Cl_2 \cdot H_2O$ [19] (ir)	$[Pd(NH_3)_4]Cl_2$ [20]		M–NH_3 [21]	
$\nu(NH_3)$	3236, 3156	3268, 3142		3000, 3300	3100–3420	3198–3326
$\delta(NH_3)_d$	1563	1601		1680, 1650, 1580	1560–1660	1550 (?), 1628
$\delta(NH_3)_s$	1325	1285		1270, 1280	1090–1360	1243, 1267, 1285
$\delta(NH_3)_r$	842	797		770–850	590–890	790–829
ν(M–N)	510	491	510 (R), 496 (ir), 468 (R)	460–530 (?)	400–540	452–524 (?)
MN bend	297	295	305 (R), 245 (ir)	270–330	240–330	

[a] Frequencies were measured from the reproduced spectrum and assigned by the present authors.

band at 1628 cm^{-1}; a shoulder at 1550 cm^{-1} may result either from factor group splitting or from the two types of positive ions. The symmetric deformation is assigned to bands at 1243 (A_1) and 1267 cm^{-1} (B_2) in the Raman spectrum and at 1243 and 1285 cm^{-1} in the infrared spectrum. The NH_3 rocking mode is expected near 800 cm^{-1}, as are bands for the nitro group and the nitrate ion. The broadness of the shoulder at 790 cm^{-1} in the infrared spectrum suggests that this may be due to the ammine groups, as opposed to the sharper band and shoulder at 824 and 829 cm^{-1} which we assign to modes of the nitro group and nitrate ion.

The NO_2 Ligand.—The Pd–NO_2 bond length is 1.984 (8) Å. As discussed previously, the nitro group appears to prefer coplanarity with Pd(2) and its ligands. However, it does show extensive vibrational motion as can be seen from the large root-mean-square thermal displacement of 0.690 Å in the $[1\bar{1}0]$ direction (Table III). As a result, the observed N–O bond distance of 1.104 ± 0.007 Å is unusually short. A correction based on a model in which O(1) rides on N(4) increases this distance to 1.305 Å, but the "riding" model is only a rough approximation and is probably overcorrecting in this case. The O–N–O and Pd–N–O bond angles of 115.2 and 122.4°, respectively, are not unusual. In KNO_2,[23] the N–O distance is 1.22 Å and the bond angle is 115.3°.

The Pd–NO_2 stretching mode (a_1) is assigned to a strong Raman band at 318 cm^{-1} (A_1). This band is strong only in the α_{zz} polarization, as expected because the stretching direction is along z. Thus the B_2 factor group component is expected to give a weak Raman band and a strong infrared band; a band at 318 cm^{-1} in the infrared spectrum is possibly this B_2 component.

The six vibrational modes of the nitro group are stretching (a_1 and b_2), deformation (a_1), wagging (b_1), rocking (b_2), and twisting (b_1) modes (Figure 4). Assignment of the internal modes of the nitro group is complicated by the similarity of its band positions with

(23) J. K. Solbakk and K. O. Stromme, *Acta Chem. Scand.*, **23**, 300 (1969).

TABLE VII

INTERIONIC DISTANCES IN $[Pd(NO_2)(NH_3)_3]_2[Pd(NH_3)_4](NO_3)_4$[a]

Atoms	Dist, Å	Multiplicity	Transformation, 2nd atom
N(1)–O(1)	3.217	1	x, y, z
N(1)–O(1)	3.788	2	$-x, y, -z$; $x, -y, -z$
N(1)–O(3)	3.068[b]	2	$1-x, y, -z$; $y, 1-x, -z$
N(1)–O(3)	3.194[b]	2	x, y, z; y, x, z
N(1)–N(5)	3.816	2	x, y, z; y, x, z
N(1)–N(5)	3.837	2	$1-x, y, -z$; $-y, x, -z$
N(2)–O(2)	3.077[b]	2	$1/2-x, 1/2+y, 1/2-z$; $1/2-y, x-1/2, 1/2-z$
N(2)–O(2)	3.287[b]	2	x, y, z; y, x, z
N(2)–Pd(2)	3.393	1	$1/2-x, 1/2+y, 1/2-z$
N(3)–O(3)	2.993[b]	4	$1/2-x, y-1/2, 1/2-z$; $x-1/2, 1/2-y, 1/2-z$; $1/2-y, x-1/2, 1/2-z$; $y-1/2, 1/2-x, 1/2-z$
N(4)–Pd(1)	3.626	1	x, y, z
N(4)–O(2)	3.826	4	x, y, z; $x-1, y, z$; y, x, z; $y, x-1, z$
N(5)–O(1)	3.253	2	x, y, z; $1-x, -y, z$
N(5)–N(2)	3.776	2	$1/2-x, y-1/2, 1/2-z$; $1/2+x, 1/2-y, 1/2-z$
N(5)–N(1)	3.816	2	x, y, z; $1-x, -y, z$
N(5)–N(1)	3.837	2	$1-x, y, -z$; $x, -y, -z$
O(1)–N(1)	3.217	1	x, y, z
O(1)–O(3)	3.334	2	x, y, z; y, x, z
O(1)–O(3)	3.437	2	x, y, z; y, x, z
O(1)–O(3)	3.658	2	$1-x, -y, z$; $-y, 1-x, z$
O(2)–O(2)	3.068	1	$1/2-y, x-1/2, 1/2-z$
O(2)–N(2)	3.077	2	$1/2-x, y-1/2, 1/2-z$; $1/2+x, 1/2-y, 1/2-z$
O(2)–N(2)	3.287	2	x, y, z; $1-x, -y, z$
O(2)–O(1)	3.334	2	x, y, z; $1-x, -y, z$
O(3)–N(3)	2.993	1	$1/2-x, 1/2+y, 1/2-z$
O(3)–N(1)	3.068	1	$1-x, y, -z$
O(3)–N(1)	3.194	1	x, y, z
O(3)–O(1)	3.437	1	x, y, z
O(3)–O(1)	3.658	1	$1-x, -y, z$
O(3)–N(2)	3.700	1	$1/2+x, 1/2-y, 1/2+z$
O(3)–O(3)′	3.776	1	$1-y, 1-x, z$

[a] Multiplicity refers to the number of times each listed interatomic distance occurs for the atom listed at the left. Estimated standard deviations for these distances are of the same order of magnitude as those given in Table V. [b] Possible disordered N–H···O interactions.

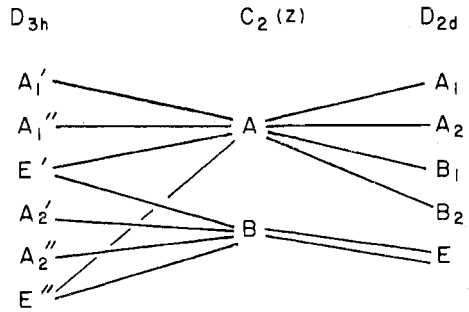

Figure 7.—Correlation diagram for NO_3^-.

those for the nitrate ion. Raman polarization and intensity data support the assignment of two bands to the nitro group, the symmetric stretching mode at 1341 cm^{-1} (A_1 and B_2) and the symmetric deformation mode at 827 cm^{-1} (A_1). In the infrared spectrum a shoulder at 1341 cm^{-1} and either a band at 824 cm^{-1} or a shoulder at 829 cm^{-1} probably result from the B_2 components. The asymmetric stretching mode (b_2) cannot be distinguished from the corresponding mode for the nitrate ion (e'). The Raman band at 1408 cm^{-1} (E) and an infrared band at either 1368 or 1408 cm^{-1} may result from the nitro group asymmetric stretching mode.

The wagging mode (b_1) of the nitro group gives a characteristic band between 550 and 650 cm^{-1} in the infrared spectrum for most complexes. The only bands measured from 350 to 700 cm^{-1} are those mentioned previously, of which at least three can be identified as Pd–NH_3 stretching modes. The fourth (555 cm^{-1}) may be the NO_2 wagging mode. $[Pd(NO_2)(NH_3)_3]Cl$[22] has a similar spectrum with several bands between 460 and 530 cm^{-1} and the next higher frequency at 770 cm^{-1}. Therefore, the NO_2 wagging mode for $Pd(NO_2)(NH_3)_3^+$ either has a frequency similar to the Pd–NH_3 stretching mode or is not detected.

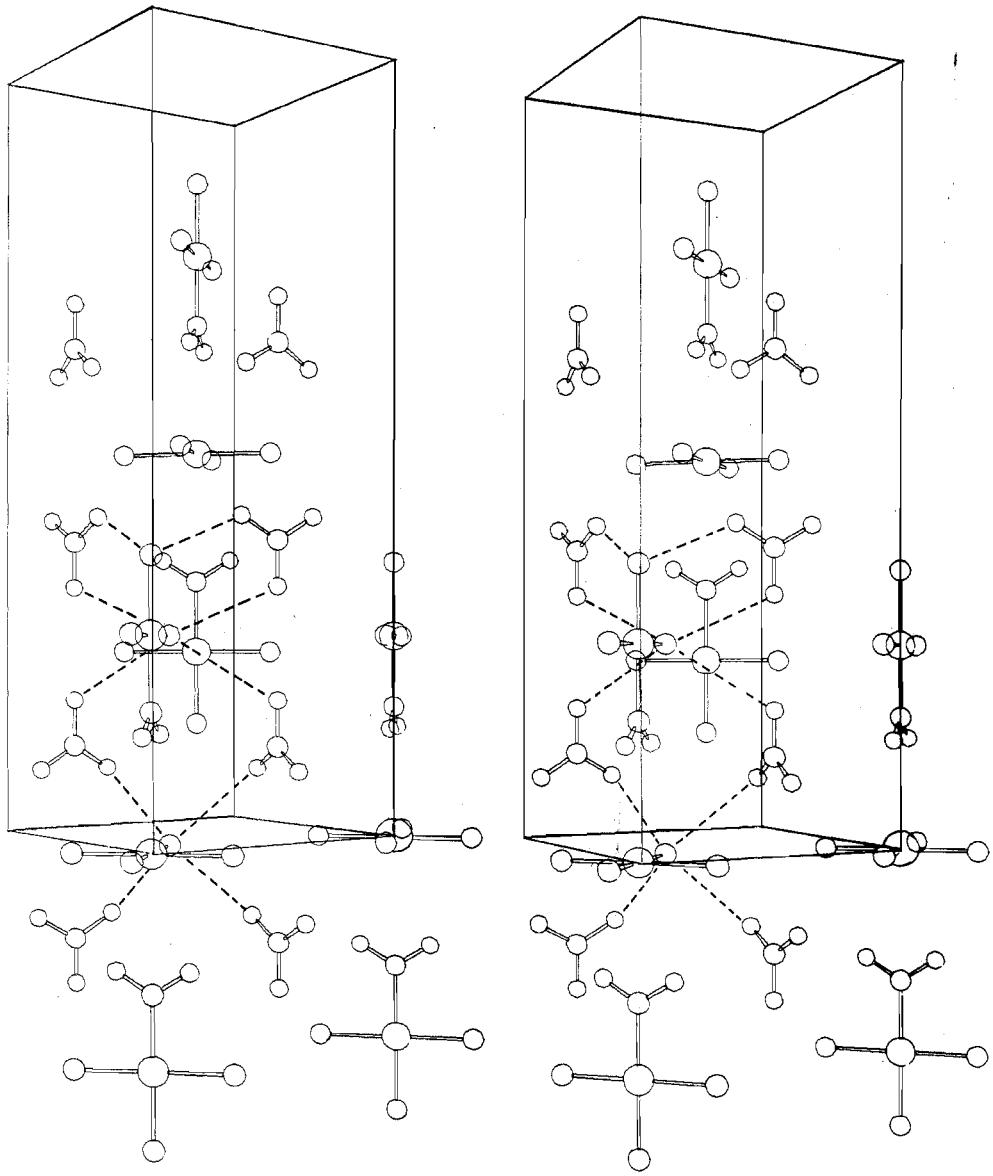

Figure 8.—A stereoview of the crystal packing in $[Pd(NO_2)(NH_3)_3]_2[Pd(NH_3)_4](NO_3)_4$. One unit cell is outlined, but the total contents of one cell are not shown, and some ions in neighboring unit cells are shown. The dashed lines show some of the closer approaches of ammine ligands to nitrate oxygens.

The Nitrate Ion.—The nitrate ions lie on $C_2(z)$ sites at $z \sim 1/8$ in the crystal and are oriented nearly parallel to the (100) and (010) planes. One N–O bond of each anion is directed along z. There are four ions in the primitive cell. The two unique bond lengths determined in the structure study, 1.230 (6) and 1.238 (6) Å, agree well with the value of 1.241 (2) Å found in $NaNO_3$.[24] Bond angles in the anion are within three standard deviations of 120°. The NO_3^- ion has four modes of vibration (Figure 7), the symmetric (a_1') and asymmetric (e′) stretching modes, the in-plane bending mode (e′), and the out-of-plane deformation (a_2'').

The symmetric stretching mode and the in-plane bending mode can be readily assigned to bands at 1052 cm^{-1} (Raman) and about 713 cm^{-1} (Raman and ir), respectively. The out-of-plane deformation is attributed to an infrared band at either 824 or 829 cm^{-1}; the other probably originates in the nitro group. The asymmetric stretching mode can be assigned to the Raman (A_1) band at 1402 cm^{-1}. Other bands in this region may arise from either the nitrate ion or the nitro ligand.

Bands in the low-frequency range may originate in the NO_2 bending and twisting modes, skeletal bending modes of the complex ions, and lattice modes. Because of the complexity of this part of the spectrum, assignment of bands to vibrational modes was not attempted.

Nonbonded Interactions.—Packing in this structure appears to be based on a combination of weak ionic attractions and disordered N–H···O interactions (see Table VII). Consider first the cations and their 2:1 stoichiometry. In Figure 8 it can be seen that the two nitrotriamminepalladium ions pack along the [001] direction so that their NO_2 groups occupy vacant axial octahedral sites around Pd(1), resulting in a monopole–dipole interaction and a coordination number of 6. Such higher coordination numbers for Pd(II) are rare but not unknown.[25] The Pd(1)–O(1) distance is 3.175 Å. The NO_2 oxygen atoms show a large thermal motion in the (110) plane suggesting a rotational disorder, constrained perhaps by the surrounding negatively charged NO_3^- anions. The axial octahedral sites for Pd(2) are occupied by NH_3 groups of neighboring nitrotriamminepalladium ions with the N(2)–Pd(2) distance of 3.393 Å suggesting a very weak ionic interaction.

Evidence for a second type of weak interaction is apparent in Table VII where four close approaches to nitrate oxygen atoms are listed for each of the three unique NH_3 groups. The geometry of the approaches, shown with dashed lines in Figure 8, places the NH_3 hydrogen atoms in positions suitable for N–H···O interactions. However, only three hydrogens are available for each set of four approaches, and these atoms would be disordered in any such system. In the case of the hydrogens of N(3) the space group *requires* disorder. The observed N–O distances range from 2.993 to 3.287 Å for these approaches, considerably shorter than the distance of approximately 3.6 Å expected in the absence of an interaction but longer than the observed values of 2.8 Å for N–H···O bonds in other structures.[26]

(24) P. Cherin, W. C. Hamilton, and B. Post, *Acta Crystallogr.*, **23**, 455 (1967).

(25) F. A. Cotton and G. Wilkinson, "Advanced Inorganic Chemistry," Interscience, New York, N. Y., 1966, p 1023.

(26) W. C. Hamilton and J. A. Ibers, "Hydrogen Bonding in Solids," W. A. Benjamin, New York, N. Y., 1968.

CONTRIBUTION FROM THE DEPARTMENT OF CHEMISTRY,
UNIVERSITY OF IOWA, IOWA CITY, IOWA 52240

The Crystal Structure of Dichlorobis(1-methyltetrazole)zinc(II)

BY NORMAN C. BAENZIGER* AND ROLAND J. SCHULTZ

Received September 29, 1969

The crystal structure of dichlorobis(1-methyltetrazole)zinc(II), $Zn(C_2N_4H_4)_2Cl_2$, has been determined at room temperature using a three-dimensional set of intensities obtained by film methods. A total of 1278 independent present reflections were collected. The unit cell is monoclinic with the following dimensions (temperature 22°): $a = 9.455 \pm 0.002$ Å, $b = 13.595 \pm 0.008$ Å, $c = 9.677 \pm 0.002$ Å; $\beta = 104.33 \pm 0.02°$; space group $P2_1/c$; $Z = 4$; $d_m = 1.66 \pm 0.02$ g cm^{-3}, $d_c = 1.68$ g cm^{-3}. The structure was refined by least-squares methods to a Hamilton's R factor of 9.7%. The coordinating ligands form a distorted tetrahedron about the zinc atom with the zinc atom being essentially planar with the tetrazole rings. The site of coordination to the tetrazole ring is the 4 position of the ring. The angles and average distances found were as follows: Zn–Cl, 2.202 ± 0.003 Å; Zn–N, 2.05 ± 0.01 Å; Cl–Zn–Cl, 118.3 ± 0.2°; N–Zn–N, 98.9 ± 0.3°.

Introduction

Various derivatives of tetrazole are able to form complexes with many metal ions.[1,2] Gilbert and Brubaker[3] reported the formation of various metal–tetrazole complexes with the general formula $M^{II}TzCl_2$ where M = Zn, Co, Pt, or Ni and Tz = 1-methyl-, 1-cyclohexyl-, or 1-phenyltetrazole. However, neither the nature of the metal–tetrazole interaction nor the coordination site of the tetrazole ring could be determined from the available experimental data. A similar difficulty in determining the nature of the interaction between vari-

(1) F. R. Benson, *Heterocycl. Compounds*, **8**, 10 (1967).
(2) D. M. Bowers and A. I. Popov, *Inorg. Chem.*, **7**, 1594 (1968).
(3) G. L. Gilbert and C. H. Brubaker, Jr., *ibid.*, **2**, 1216 (1963).